Cell Reports
Physical Science

CellPress
OPEN ACCESS

Article

P-stereogenic *N*-vinylphosphonamides enabled by asymmetric allylic substitution-isomerization

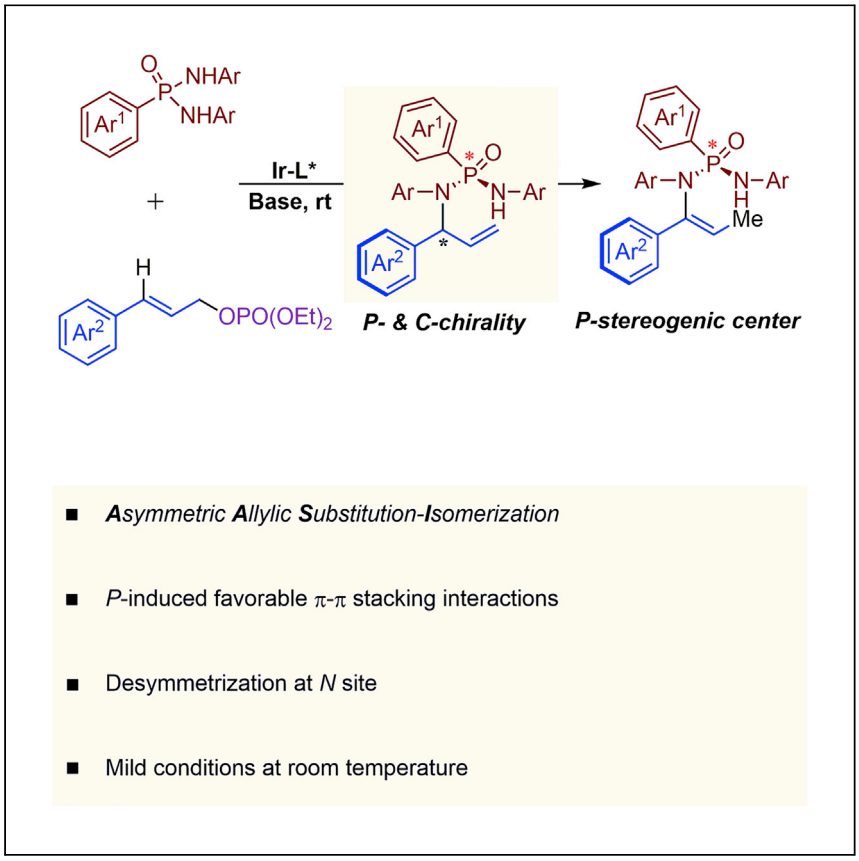

Zhang et al. report a highly enantioselective synthesis of *P*-stereogenic *N*-vinylphosphonamides using an *asymmetric allylic substitution-isomerization* (*AASI*) strategy. The efficient catalytic approach provides rapid access to a wide range of enantioenriched *N*-vinylphosphonamides. Computational studies demonstrate that the *P*-stereogenic center induces more favorable π-π stacking interactions in *N*-vinylphosphonamides.

Xiu-Lian Zhang, Xiaotian Qi, Ying-Xiang Wu, Peng Liu, Ying He

pengliu@pitt.edu (P.L.)
yhe@njust.edu.cn (Y.H.)

Highlights

Asymmetric allylic substitution-isomerization (AASI) strategy

Asymmetric desymmetrization of phosphorus compounds at *N* site

Facile access to *P*-stereogenic *N*-vinylphosphonamides

Zhang et al., Cell Reports Physical Science 2, 100594
October 20, 2021
https://doi.org/10.1016/j.xcrp.2021.100594

Cell Reports
Physical Science

CellPress
OPEN ACCESS

Article

P-stereogenic *N*-vinylphosphonamides enabled by asymmetric allylic substitution-isomerization

Xiu-Lian Zhang,[1] Xiaotian Qi,[2] Ying-Xiang Wu,[1] Peng Liu,[2,*] and Ying He[1,3,*]

SUMMARY

The catalytic and stereoselective synthesis of *P*-stereogenic compounds has drawn a lot of attention, since these compounds possess widespread applications in organic synthesis. Thus, novel strategies for the construction of new complex *P*-chiral molecules still need to be developed. Here, we report a highly enantioselective synthesis of *P*-stereogenic *N*-vinylphosphonamides using an *asymmetric allylic substitution-isomerization* (*AASI*) strategy. The efficient catalytic approach provides rapid access to a wide range of enantioenriched *N*-vinylphosphonamides in up to 85% yields and 99:1 enantiomeric ratio. Computational studies demonstrate that the *P*-stereogenic center induces more favorable π-π stacking interactions in *N*-vinylphosphonamides.

INTRODUCTION

Enantioenriched *P*-stereogenic phosphorus compounds have extensive applications in a number of fields, including biochemistry,[1–4] pharmaceutical chemistry,[5,6] and asymmetric organic synthesis.[7–15] Among these, phosphorus-nitrogen compounds have received a steadily growing interest from the pharmaceutical industry, as exemplified by phosphoramidated drugs Sofosbuvir, Stampidine, and phosphonamidated marketed drug Tenofovir alafenamide (Figure 1). Of particular note, Remdesivir, initially developed by Gilead to treat Ebola virus, has attracted much attention because it has shown a certain value in the treatment of the COVID-19 infections (Figure 1A).[16] Thus, the development of catalytic strategies for accessing *P*-stereogenic architectural molecules is highly desirable.

Over the years, methodologies for the preparation of *P*-stereogenic molecules were reported, which mainly relied on desymmetrization of prochiral phosphorus compounds[17–32] and kinetic resolution of racemic phosphorus compounds,[33–35] as well as arylation, alkylation, or alkenylation of secondary phosphine oxides (Figure 1B).[36–46] In specific cases, the simultaneous demand of stereochemistry at both phosphorus and carbon atoms in the prodrugs put up a big challenge to the catalytic synthesis of *P*- and *C*-chiral compounds (Figure 1A).[47–51] Consequently, recent catalytic approaches have been developed by the intermolecular coupling or addition reactions between phosphorus(V) compounds and internal olefins.[52–61] Despite much progress, to the best of our knowledge, whether the enantioselective desymmetrization of phosphorus compounds takes place at the *N* site rather than the *C* or *O* sites is still unknown (Figure 1B).

Recently, our group reported an *asymmetric allylic substitution-isomerization* (*AASI*) strategy for the synthesis of axially chiral enamides and styrenes in excellent yields

[1]School of Chemistry and Chemical Engineering, Nanjing University of Science & Technology, Nanjing 210094, China

[2]Department of Chemistry and Department of Chemical and Petroleum Engineering, Pittsburgh, PA 15260, USA

[3]Lead contact

*Correspondence: pengliu@pitt.edu (P.L.), yhe@njust.edu.cn (Y.H.)

https://doi.org/10.1016/j.xcrp.2021.100594

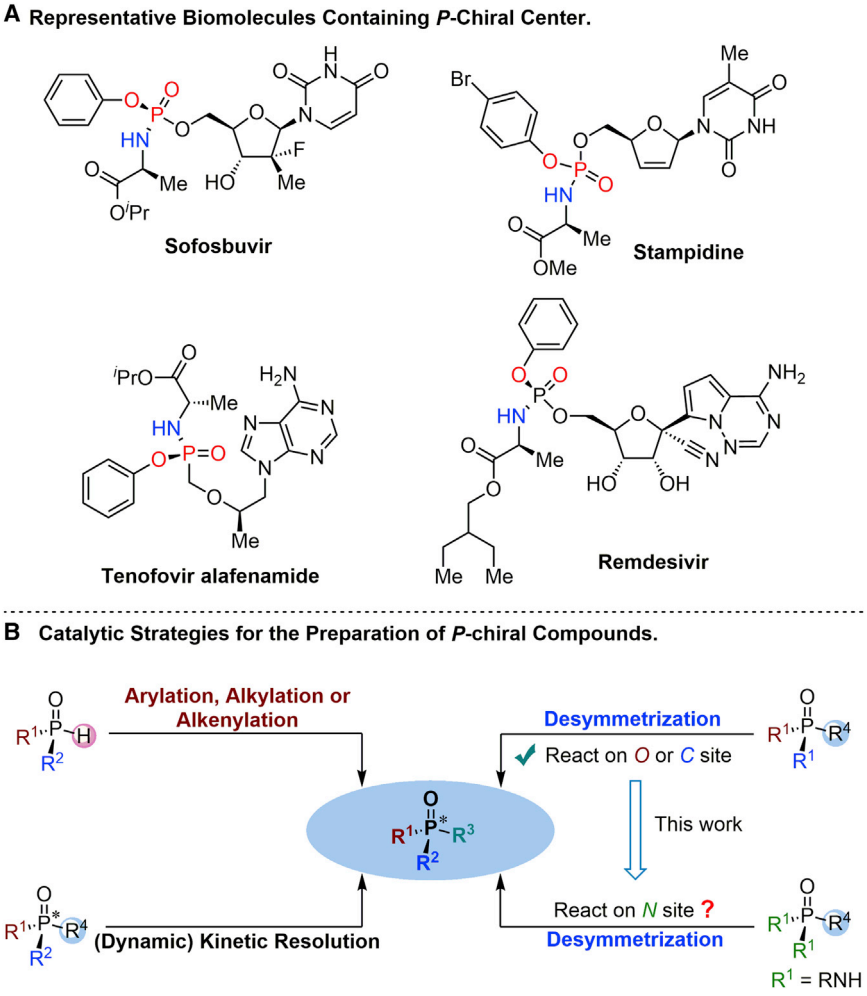

Figure 1. Representative *P*-stereogenic compounds and their synthetic strategies

(A) Representative biomolecules containing *P*-chiral center.

(B) Catalytic strategies for the preparation of *P*-chiral compounds.

with high enantioselectivities (Figures 2A and 2B).[62–64] The mechanistic studies of *AASI* revealed that the reaction proceeds via a pathway in which isomerization is the terminal reaction, occurring after the iridium-catalyzed AAS.[65–72] The stereospecific isomerization process, however, proceeded through completely different pathways to accomplish the central-to-axial chirality transfer. For the base-promoted isomerization (1,3-proton transfer), deprotonation of allylic products at the benzylic position first occurred to afford chiral ion-pair intermediates. This chiral ion-pair would then generate to axially chiral enamides via central-to-axial chirality transfer. In this context, the H-bonding interaction-assisted central-to-axial chirality transfer ensured the high enantioselectivities of axially chiral enamides (Figure 2A, route 1). As for the iridium-catalyzed isomerization of enantioenriched allylic products (1,3-hydride transfer), the central-to-axial chirality transfer was achieved through the iridium-catalyzed benzylic C-H oxidative addition and C-H reductive elimination. The hydroxyl of naphthol is critical for the stereospecificity because the coordination of the deprotonated hydroxyl with Ir prevents the rotation around the C-C axis (Figure 2A, route 2). In both cases, kinetically controlled isomerizations were demonstrated by experimental and computational studies.[73,74]

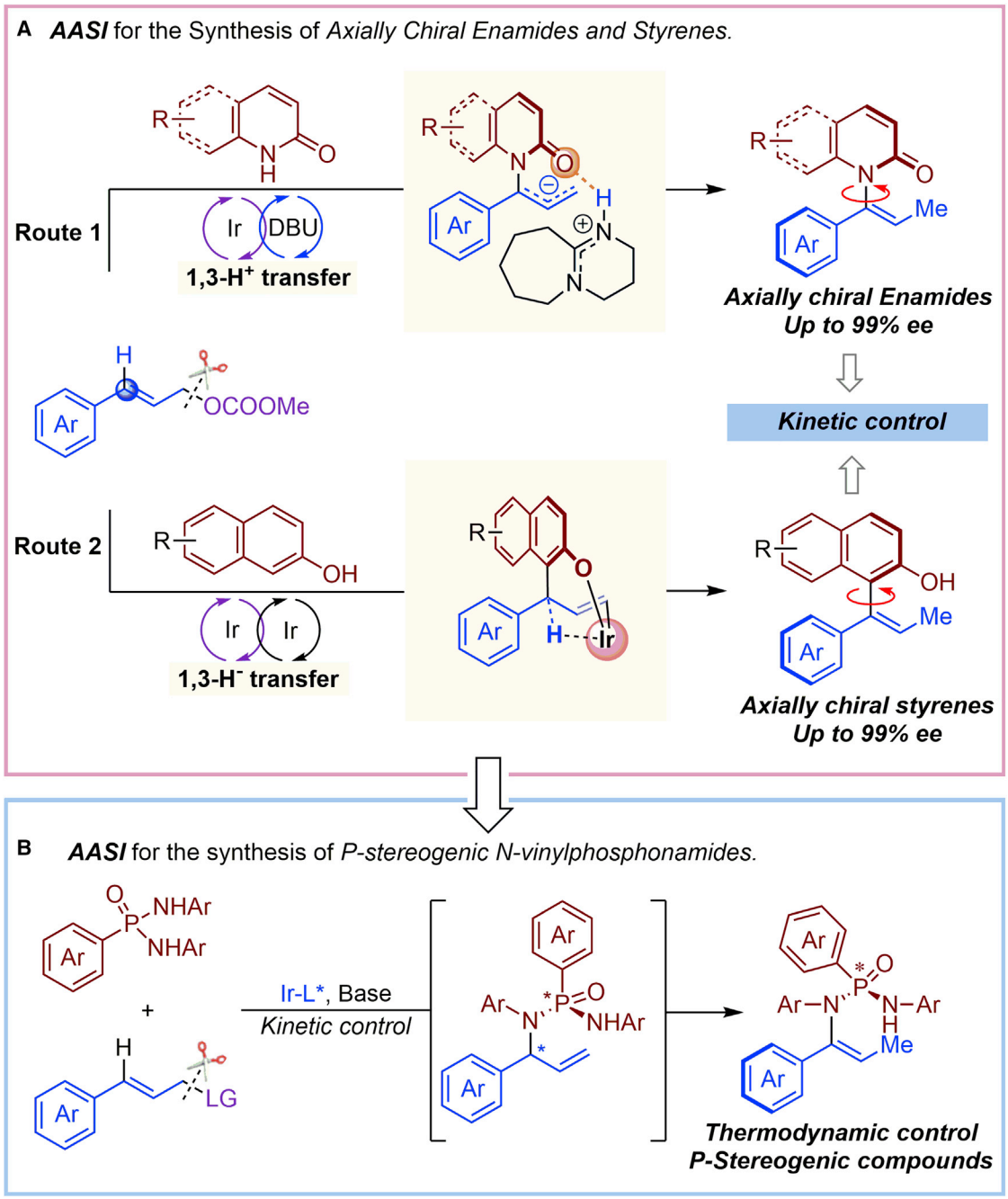

Figure 2. Asymmetric allylic substitution-isomerization (AASI)
(A) AASI for the synthesis of axially chiral enamides and styrenes.
(B) AASI for the synthesis of *P*-stereogenic *N*-vinylphosphonamides.

Inspired by these results, we envision that the *AASI* strategy could be utilized to take the challenge of synthesizing *P*-stereogenic compounds (Figure 2B). With phosphonamide and cinnamyl carbonate as the reactants, *P*- and *C*-stereogenic centers could be generated simultaneously in the first step, and then base or iridium mediated 1,3-H transfer would establish an N-C axis to afford chiral *N*-vinylphosphonamides. We assume that the *P*-stereogenic center would enable the compounds either

configurationally stable atropisomers or diastereomeric confomers about the N-C axis under thermodynamic control[75–82] (Figure 2B). To the best of our knowledge, the thermodynamic control using *P*-stereogenic center to induce atropisomers or conformers are underdeveloped regions in asymmetric synthesis. Nevertheless, at the outset of our studies, we anticipate the momentous challenge of finding conditions to achieve our goal will be that the products must be obtained with high enantioselectivity, regioselectivity, and geometrical (*Z*/*E*) selectivity simultaneously.

RESULTS AND DISCUSSION

Optimized conditions

The initial feasibility of the desymmetrization reaction was explored with cinnamyl carbonate **1** and phosphonamide **2** under conditions similar to our previous report.[62] It should be noted that if the enantioselective desymmetrization happens, it would represent the rare example of desymmetrization of phosphorus compounds via asymmetric vinylation. First, the amount of phosphonamide and base were strictly controlled to avoid overreaction between phosphonamide and cinnamyl carbonate. Several phosphoramidite ligands were tested, fortunately affording the desired *P*-stereogenic *N*-vinylphosphonamide **3**, albeit with low yields and an enantiomeric ratio (e.r.) (Table 1, entries 1–6). By choosing the best ligand **L1**, we then screened the effects of the base and found it had a certain influence on reactivity and enantioselectivity of the reaction (entries 7–11), in which KHMDS gave the best e.r. value and moderate yield (entry 8). The leaving groups of **1** such as -OBoc and -Cl led to diminished yields and lower e.r. values of 65:35 and 75:25, respectively (entries 12 and 14). A relatively high enantioselectivity but dramatically low yield of 25% was obtained using -OBz as the leaving group in substrate **1** (entry 15). It's comforting that the screening of leaving group $-OPO(OEt)_2$ in substrate **1** provided the target product in a moderate yield with 84:16 e.r. (entry 13). Changing the solvent to toluene resulted in a moderate yield and higher enantioselectivity (89:11 e.r.). The use of other leaving groups in **1** was proved to have a low efficiency in reactivity of the reactions (entries 17 and 18). In order to break the bottlenecks, we anticipated that enhancing the steric hindrance adjacent to phosphorus center of **2** may be beneficial to the reaction. Gratifyingly, the simple introduction of the *o*-Me group gave us a high enantioselectivity (95.5:4.5 e.r.) with an 80% isolated yield of **3a** (entry 20).

Substrate scope of the reaction

With the aforementioned optimized conditions, we set out to explore the substrate generality of the reaction. As shown in Figure 3, a series of cinnamyl phosphates, readily prepared from the corresponding cinnamyl alcohol, could smoothly undergo the *N*-vinylation. The aryl substituted with electron-neutral (**H**), electron-withdrawing (**Cl** and **Br**), and electron-donating (**Ph**) groups at the *para*-position were well-tolerated under standard conditions in which the corresponding products were afforded in 92:8 to 99:1 e.r. values (Figure 3, **3a–3c**, **3e**). However, when the arene ring has a strong electron-withdrawing group such as *p*-nitro substitution, the product **3d** was obtained in a low yield of 14% and 85:15 e.r. The reaction allowed for the compatibility of various substituents at *meta*- and *othro*-positions in arenes rings of **1**, affording the corresponding products in 86:14 to 94:6 e.r. (**3f**-**3i**), albeit with a low yield of **3j**. The difunctionalized substrate was also compatible with the reaction, as exemplified by the difluoro substituted cinnamyl phosphate, furnishing the desired product **3k** in a moderate yield with slightly decreased enantioselectivity. Moreover, the fused-aryl type substrates of **1**, including 1-naphthyl and 2-naphthyl substituents, tolerated the desymmetrization, delivering products **3l** and **3m** in 89:11 e.r. and 92:8 e.r., respectively. It is valuable to note that the reaction was not limited to aryl moieties of substrate **1**. Strikingly, thienyl and furyl substituted methyl

Table 1. Optimized conditions

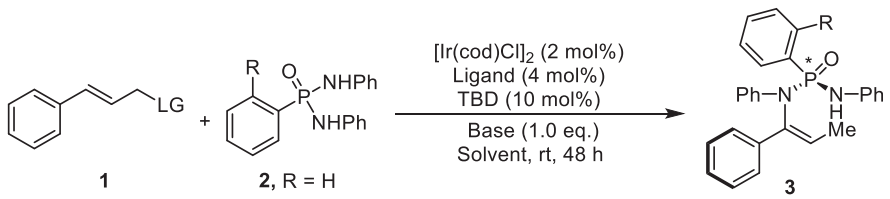

1 2, R = H 3

Entry	Ligand	Base	Leaving group	Solvent	Yield (%)	e.r.
1	L1	DBU	OCOOMe	THF	28	78:22
2	L2	DBU	OCOOMe	THF	58	68:32
3	L3	DBU	OCOOMe	THF	20	51:49
4	L4	DBU	OCOOMe	THF	17	67:33
5	L5	DBU	OCOOMe	THF	20	59:41
6	L6	DBU	OCOOMe	THF	35	74:26
7	L1	DABCO	OCOOMe	THF	13	66:34
8	L1	KHMDS	OCOOMe	THF	41	81:19
9	L1	TBD	OCOOMe	THF	35	80:20
10	L1	LiHMDS	OCOOMe	THF	36	79:21
11	L1	NaHMDS	OCOOMe	THF	32	80:20
12	L1	KHMDS	OBoc	THF	14	65:35
13	L1	KHMDS	$OPO(OEt)_2$	THF	45	84:16
14	L1	KHMDS	Cl	THF	24	75:25
15	L1	KHMDS	OBz	THF	25	82:18
16	L1	KHMDS	$OPO(OEt)_2$	toluene	52	89:11
17	L1	KHMDS	OCOOMe	toluene	16	89:11
18	L1	KHMDS	OBz	toluene	25	86:14
19[a]	L1	KHMDS	OCOOMe	toluene	70	95:5
20[a]	L1	KHMDS	$OPO(OEt)_2$	toluene	80	95.5:4.5

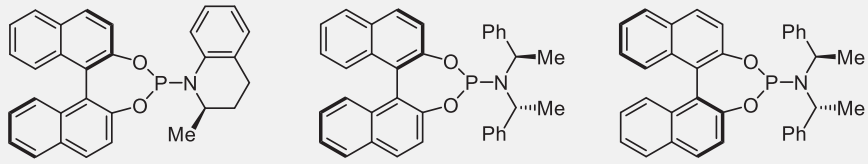

(*R*,*R*)-**L1** (*R*,*R*,*R*)-**L2** (*S*,*R*,*R*)-**L3**

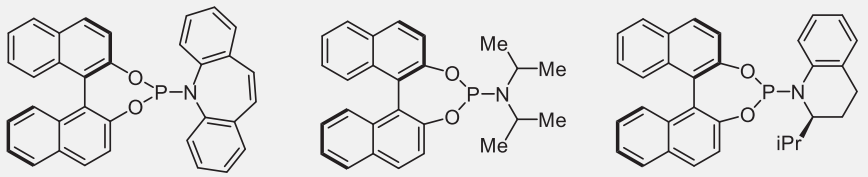

(*R*)-**L4** (*R*)-**L5** (*R*,*R*)-**L6**

Reaction conditions, 1 (0.1 mmol), 2 (0.15 mmol), $[Ir(cod)Cl]_2$ (2 mol%), ligand (4 mol%), 1,5,7- triazabicyclo[4.4.0]dec-5-ene (TBD) (10 mol%), base (0.1 mmol), solvent (1.0 mL), room temperature for 48 h, argon atmosphere, isolated yields, and enantiomeric ratio (e.r.) values were determined by chiral HPLC.
[a]R = Me, the product was obtained >19:1 diastereomeric ratio (d.r.) by ^1H NMR.

carbonates were found to be suitable for the reaction (**3n** and **3o**). The absolute stereochemistry of **3a** was determined by X-ray crystallography and that of the other products were assigned by analogy.

Although bulky groups adjacent to the phosphorus center are beneficial for e.r. values of products **3**, we are eager to know whether other substituents tolerate

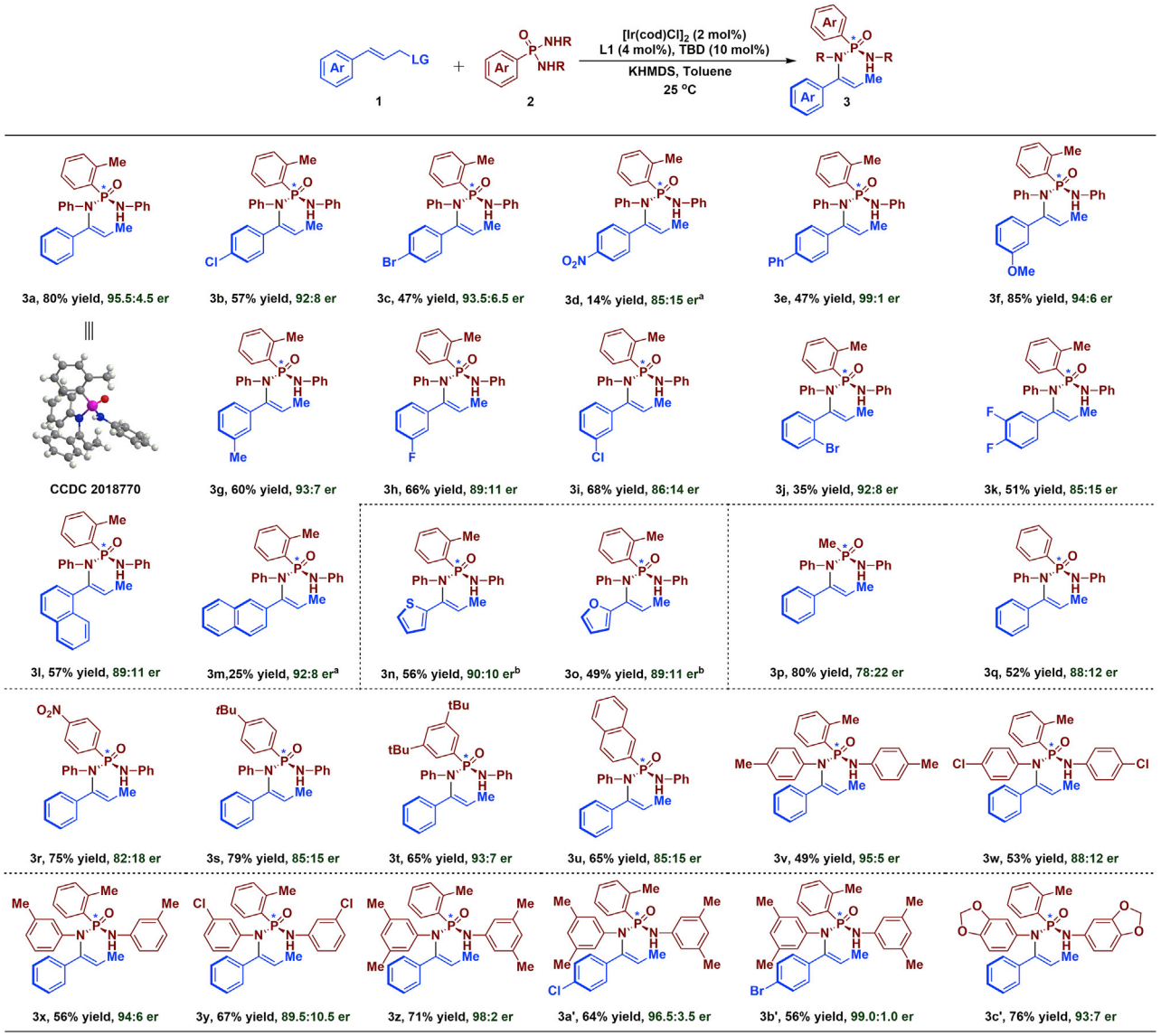

Figure 3. Substrate scope of the reaction

Reaction conditions, **1** LG = $OPO(OEt)_2$ (0.1 mmol), **2** (0.15 mmol), $[Ir(cod)Cl]_2$ (2 mol%), L1 (4 mol%), ,5,7- triazabicyclo[4.4.0]dec-5-ene (TBD; 10 mol%), KHMDS (0.1 mmol), toluene (1.0 mL), room temperature for 48 h, argon atmosphere, isolated yields, and e.r. values were determined by chiral high-performance liquid chromatography (HPLC).

[a]The reaction was proceeded at room temperature for 72 h.

[b]LG = OCOOMe.

under our optimized conditions. Considering both the electronic and steric effects, different phosphonamides were prepared and subjected to the desymmetrization. As displayed in Figure 3, we found that the catalysis system was applicable to various phosphonamides bearing different types of substituents adjacent to phosphorus center (**3p–3u**) and acceptable e.r. were obtained. However, the substrate with the methyl group adjacent to the phosphorus center affords the product an 80% yield but moderate e.r. of 78:22.

It's not surprising that phosphonamides featuring different amines have distinct reactivity and enantioselectivity since the desymmetrization occurs at the nitrogen

atom. Substrates with an electron-donating group (Me) on the phenyl ring proceeded smoothly to give the products in high e.r. up to 95:5 (**3v** and **3x**). Substrates bearing an electron-withdrawing group (Cl) at the *para*- and *meta*-positions of the phenyl rings have a negative effect in enantioselectivity, and 88:12 and 89.5:10.5 e.r. of products were obtained, respectively (**3w** and **3y**). Moreover, the phosphonamides substituted with 3,5-dimethyl amine provide enhanced reaction performances, especially in terms of enantioselectivity, delivering enantioenriched products in 96.5:3.5 to 99.0:1.0 e.r. with 56%–71% yield (**3z–3b′**). It was somewhat satisfying to find that phosphonamides bearing 3,4-(methylenedioxy)aniline were also tolerable under the optimal conditions, providing the corresponding product **3c′** a 76% yield with 93:7 e.r.

Mechanistic studies

The X-ray crystal structure of **3a** (*vide supra*) possesses two stereogenic elements: the stereogenic center at the *P* atom has an (*R*) absolute configuration and the chiral axis at the C–N bond of the alkenyl amine has an (S_a) configuration. While the *P*-stereocenter is formed in the Ir-catalyzed enantioselective allylation step, the (S_a) configuration of the chiral axis in the crystal structure of **3a** may be due to two possible mechanistic scenarios. If the atropisomer is configurationally stable (i.e., the rotation about the C–N bond is restricted at room temperature), the axial chirality should be determined in a stereospecific central-to-axial chirality transfer in the 1,3-H transfer step (Figure 4A).[62] On the other hand, if the two diastereoisomeric atropisomers can interconvert via free rotation about the C–N bond at room temperature, the observed (S_a)-chiral axis should be simply because this atropisomer is thermodynamically more stable than the (R_a) atropisomer. To investigate which scenario was involved, we performed density functional theory (DFT) calculations to investigate the rotation about the C–N bond in **3a** to form **3aa** and how the newly constructed *P*-stereogenic center affects the relative thermodynamic stability of this pair of diastereoisomeric atropisomers (Figure 4B). All the structures were optimized at the M06-2X/6-31G(d)[83] level of theory. Both DLPNO-CCSD(T)/def2-TZVP[84–86] and M06-2X/6-311+G(d,p) were used to calculate single-point energies in toluene with the SMD[87] solvation model. The rotation about the C–N axis in **3a** occurs through the transition state **TS-1**, which requires a low activation-free energy of only 13.2 kcal/mol using DLPNO-CCSD(T) and 14.7 kcal/mol using M06. Moreover, **3aa** is 2.1 and 2.8 kcal/mol less stable than **3a** at the level of theory. These computational results indicate that the isomerization via C–N bond rotation is kinetically facile under the experimental conditions. Thus, the observed (S_a) configuration in diastereoisomeric atropisomer **3a** is under thermodynamic control because **3a** is more stable than other atropisomer **3aa**. The calculated ratio of **3a** to **3aa** (97:3) is consistent with the experimental results (Figure 3, single diastereomer of **3a** was obtained). Structural analyses show that **3a** is stabilized by the π-π stacking interaction between the *P*-anilinyl group and the phenyl group in the alkenyl moiety of the enamide (Figure 4B). The distances between the parallel displaced aryl rings (~3 Å) further corroborate the existence of the π-π stacking interaction.[88–90] The π-π stacking interaction is much weaker in **3aa** because the newly generated N-C axis points the phenyl group further away from the *P*-anilinyl group (>3.5 Å). Therefore, the computational results demonstrate that the *P*-stereogenic center induced more favorable π-π stacking interactions in **3a**, leading to the greater stability of **3a** (see DFT-calculated details in Tables S1–S3). It should be noted that the reaction of a phosphonamide possessing an alkyl group (^{n}Pr) on the nitrogen atoms did not afford an optically active product (**3d′**, <2% ee), thus leading to the hypothesis of favorable π-π stacking interactions between the aryl moiety present on the nitrogen of the phosphonamide and the aryl group on the allylic electrophile in the transition state

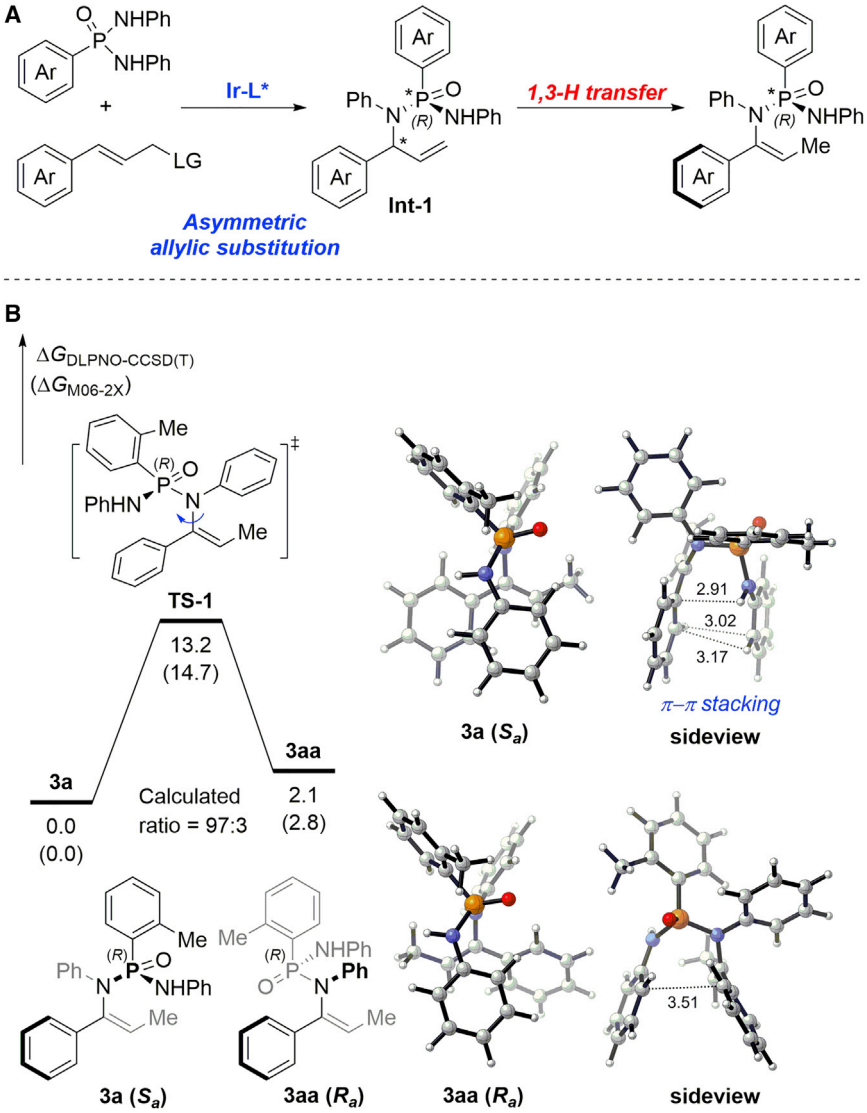

Figure 4. Density functional theory (DFT) calculations

(A) General pathway for the formation of *N*-vinylphosphonamide through Ir-catalyzed AAS and 1,3-H transfer. LG = $OPO(OEt)_2$.

(B) Computational studies of the isomerization between diastereoisomeric atropisomers **3a** and **3aa**. All energies are in kcal/mol. Bond lengths are in angstrom. $S_a = S_{axial}$, $R_a = R_{axial}$.

of the enantiodetermining step of the allylic substitution (creation of the *P*, *C*-stereogenic centers) (see Supplemental information for detailed characterization of **3d'**). Although attempts to isolate **int-1** failed, we proposed that the isomerization process was promoted by base instead of iridium because of the relatively more acidic allylic C-H bond in **int-1**.

Synthetic transformations

To evaluate the reliability of this catalytic methodology for preparing *P*-stereogenic *N*-vinylphosphonamides in preparative synthesis, scale-up synthesis was examined under the optimal reaction conditions but with the catalyst loading halved (Figure 5A). To our delight, the desired product **3a** was obtained in a moderate yield

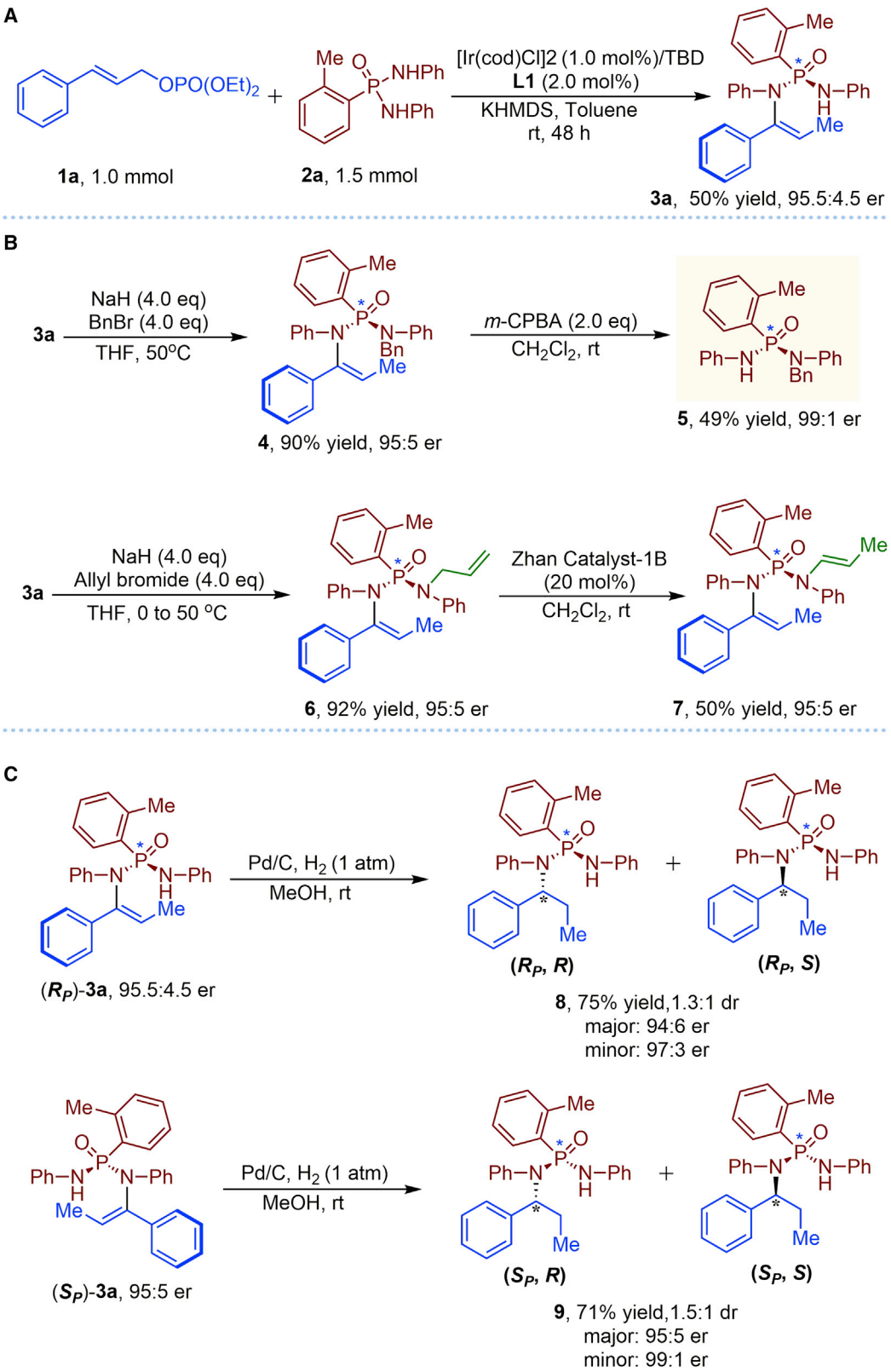
A
OPO(OEt)2
1a, 1.0 mmol
NHPh
NHPh
2a, 1.5 mmol
[Ir(cod)Cl]2 (1.0 mol%)/TBD
L1 (2.0 mol%)
KHMDS, Toluene
rt, 48 h
3a, 50% yield, 95.5:4.5 er
B
3a
NaH (4.0 eq)
BnBr (4.0 eq)
THF, 50°C
4, 90% yield, 95:5 er
m-CPBA (2.0 eq)
CH2Cl2, rt
5, 49% yield, 99:1 er
NaH (4.0 eq)
Allyl bromide (4.0 eq)
THF, 0 to 50 °C
6, 92% yield, 95:5 er
Zhan Catalyst-1B
(20 mol%)
CH2Cl2, rt
7, 50% yield, 95:5 er
C
(RP)-3a, 95.5:4.5 er
Pd/C, H2 (1 atm)
MeOH, rt
(RP, R)
(RP, S)
8, 75% yield,1.3:1 dr
major: 94:6 er
minor: 97:3 er
(SP)-3a, 95:5 er
Pd/C, H2 (1 atm)
MeOH, rt
(SP, R)
(SP, S)
9, 71% yield,1.5:1 dr
major: 95:5 er
minor: 99:1 er

of 50% while maintaining its enantioselectivity (95.5:4.5 e.r.). Synthetic transformations were then carried out. Treatment of **3a** with BnBr afforded product **4** in a high yield and with enantioselectivity maintained (95:5 e.r.). The oxidative cleavage reaction then occurred to generate the enantioenriched phosphonamide **5** in 99:1 e.r. with 49% yield (Figure 5B, top). The allyl group could also be introduced into **3**, affording product **6** in a 92% yield with 95:5 e.r. An unprecedented isomerization occurred to generate **7** in an excellent yield without any loss in its enantioselectivity (Figure 5B, bottom). At last, the straightforward reduction of **3a** was carried out to afford *P*- and *C*-stereogenic compounds. To our delight, the reaction proceeded smoothly, generating two isomers (R_P, *R*)-**8** and (R_P, *S*)-**8** in both high enantioselectivities of 94:6 and 97:3 e.r. with a 75% total yield (Figure 5C, top). Encouraged by this result, (S_P)-**3a** was then synthesized and subjected to the reduced reaction, which afforded (S_P, *R*)-**9** and (S_P, *S*)-**9** in 95:5 and 99:1 e.r. with a 71% total yield (Figure 5C, bottom). These results highlight the importance of the strategy for the preparation of *P*-stereogenic *N*-vinylphosphonamides, which could be used to synthesize all four possible stereoisomers by a simple reduction. A similar result could also be observed with regard to other *P*-stereogenic *N*-vinylphosphonamides **3** (see Supplemental information for details).

Applications

At last, because of the catalytic nature of phosphonamide compounds, we turned our attention to asymmetric reactions using *P*-stereogenic *N*-vinylphosphonamides as chiral catalysts. Using **3a** as the catalyst, the enantioselective iodocyclization for the construction of chiral chromans was carried out in which a 56% yield and 60.5:39.5 e.r. of **11** was obtained (Figure 6A). The enantioselective reductive aldol reactions between enone **12** and benzaldehyde afforded product **13** in high diastereomeric ratio (d.r.) of 93:7 albeit with 55.5:44.5 e.r. in the presence of catalyst **5**. A moderate yield with relatively low d.r. and e.r. of **13** was obtained when the reaction proceeded at −30°C using **3a** as the catalyst (Figure 6B).

In conclusion, the desymmetrization of phosphonamides at the *N* atom enabled by *AASI* has been developed, leading to *P*-stereogenic *N*-vinylphosphonamides in good yields with excellent enantioselectivities. The protocol allows for the facile construction of *P*-stereogenic *N*-vinylphosphonamides under both kinetic and thermodynamic control. Importantly, the *P*-stereogenic *N*-vinylphosphonamides could be easily reduced, which generated all four stereoisomers in high enantioselectivity. Moreover, the obtained chiral *N*-vinylphosphonamides could be used as catalysts for several asymmetric transformations. Extension of this methodology to other challenging new molecules is currently underway in our laboratory.

EXPERIMENTAL PROCEDURES

Resource availability

Lead contact

Further information and requests for resources and reagents should be directed to and will be fulfilled by the lead contact, Ying He (yhe@njust.edu.cn).

Materials availability

Commercially available reagents were used without further purification.

Figure 5. Synthetic transformations

(A) A large-scale experiment.

(B) Synthetic transformations of **3a**.

(C) Reduction of (R_P)-**3a** and (S_P)-**3a**.

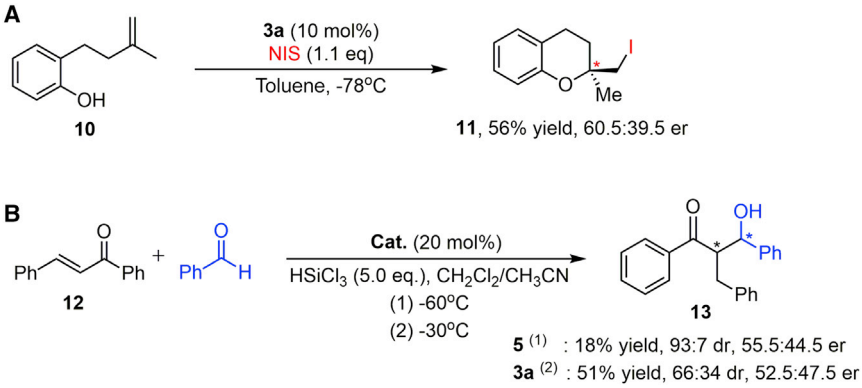

Figure 6. Applications of *P*-stereogenic *N*-vinylphosphonamides

(A) Enantioselective iodocyclization using **3a** as a catalyst.

(B) Enantioselective reductive aldol reactions catalyzed by **5** and **3a**, respectively.

Data and code availability

The authors declare that data supporting the findings of this study are available within the article and the Supplemental information files. The calculated data of 3q and 4 are shown in Figure S1 and Tables S4–S9. The X-ray crystallographic coordinate for the structure reported in this study has been deposited at the Cambridge Crystallographic Data Centre (CCDC) under deposition number CCDC 2018770 (3a) (see crystallographic details in Tables S10–S15). These data can be obtained free of charge from the CCDC via https://www.ccdc.cam.ac.uk/structures/.

Materials and characterization

Unless otherwise noted, all starting materials were purchased from commercial sources and used without any further purification. The reactions were carried out in the glovebox unless otherwise stated. Toluene, DMF (*N*,*N*-dimethylformamide), DCM (dichloromethane), and DCE (1,2-dichloroethane) were obtained from commercial sources. Anhydrous THF (tetrahydrofuran) is obtained by distillation over sodium and benzophenone ketyl immediately before use. Chemicals were used as obtained from the suppliers. The analytical data for the known compounds were found to match with the literature data and stored at −30°C under an inert atmosphere. Room temperature is 23°C–25°C. TLC plates were visualized under UV light (254 nm). ^{1}H NMR, ^{19}F NMR, ^{13}C NMR, and ^{31}P spectra were recorded on Bruker-AVANCE 500 spectrometer, and chemical shifts are reported in ppm. Multiplicities are reported using the following abbreviations: s, singlet; d, doublet; t, triplet; q, quartet; m, multiplet. High-resolution mass spectral data were acquired on Agilent Technologies Accurate-Mass Q-TQF LC/MS 6520, operated by China Pharmaceutical University. e.r. and d.r. were determined on a Thermo Fisher UltiMate 3000 Chiral HPLC using AD, OD, ID, IA, and IC columns and ^{1}H NMR. For full details of the synthesis and characterization of compounds, see the Supplemental experimental procedures and Figures S2–S234.

SUPPLEMENTAL INFORMATION

Supplemental information can be found online at https://doi.org/10.1016/j.xcrp.2021.100594.

ACKNOWLEDGMENTS

We gratefully acknowledge the financial support from the Natural Science Foundation of Jiangsu Province (BK20180447), the Fundamental Research Funds for the

Central Universities (30918011313 and 30919011273), and the NSF (CHE1707490). P.L. and X.Q. thank the University of Pittsburgh and the National Science Foundation (CHE1654122) for financial support of the computational work. DFT calculations were performed at the Center for Research Computing at the University of Pittsburgh, the Texas Advanced Computing Center (TACC) at The University of Texas at Austin, and the Extreme Science and Engineering Discovery Environment (XSEDE), supported by the National Science Foundation grant number ACI-1548562. We especially thank Prof. Yi-Ming Wang (University of Pittsburgh) for helpful suggestions in the preparation of the manuscript.

AUTHOR CONTRIBUTIONS

Y.H. and P.L. directed the research. X.-L.Z. and Y.-X.W. performed the experiments and prepared the Supplemental information. X.Q. performed the DFT studies. The manuscript was written with contributions of all authors.

DECLARATION OF INTERESTS

X.-L.Z. and Y.H. are listed as inventors on a Chinese patent application describing the synthesis of compound 5 (application number: 2021108080095).

Received: July 10, 2021
Revised: July 28, 2021
Accepted: September 2, 2021
Published: October 1, 2021

REFERENCES

1. Kudzin, Z.H., Kudzin, M.H., Drabowicz, J., and Stevens, C.V. (2011). Aminophosphonic acids-phosphorus analogues of natural amino acids. part 1: syntheses of α-aminophosphonic acids. Curr. Org. Chem. *15*, 2015–2071.

2. Horsman, G.P., and Zechel, D.L. (2017). Phosphonate Biochemistry. Chem. Rev. *117*, 5704–5783.

3. Petkowski, J.J., Bains, W., and Seager, S. (2019). Natural products containing 'rare' organophosphorus functional groups. Molecules *24*, 866.

4. Focken, T., and Hanessian, S. (2014). Application of cyclic phosphonamide reagents in the total synthesis of natural products and biologically active molecules. Beilstein J. Org. Chem. *10*, 1848–1877.

5. Mucha, A., Kafarski, P., and Berlicki, Ł. (2011). Remarkable potential of the α-aminophosphonate/phosphinate structural motif in medicinal chemistry. J. Med. Chem. *54*, 5955–5980.

6. Pradere, U., Garnier-Amblard, E.C., Coats, S.J., Amblard, F., and Schinazi, R.F. (2014). Synthesis of nucleoside phosphate and phosphonate prodrugs. Chem. Rev. *114*, 9154–9218.

7. Huber, R., Passera, A., and Mezzetti, A. (2019). Which future for stereogenic phosphorus? Lessons from P* pincer complexes of iron(ii). Chem. Commun. (Camb.) *55*, 9251–9266.

8. Cabré, A., Riera, A., and Verdaguer, X. (2020). *P*-stereogenic amino-phosphines as chiral ligands: from privileged Intermediates to asymmetric catalysis. Acc. Chem. Res. *53*, 676–689.

9. Kuwabara, K., Maekawa, Y., and Murai, T. (2020). *P*-stereogenic phosphinothioic acids, phosphonothioic acids and their esters: syntheses, reactions, and applications. Tetrahedron *76*, 131152.

10. Su, H.Y., and Taylor, M.S. (2017). *P*-stereogenic β-aminophosphines: preparation and applications in enantioselective organocatalysis. J. Org. Chem. *82*, 3173–3182.

11. Xu, G., Senanayake, C.H., and Tang, W. (2019). *P*-chiral phosphorus ligands based on a 2,3-dihydrobenzo[d][1,3]oxaphosphole motif for asymmetric catalysis. Acc. Chem. Res. *52*, 1101–1112.

12. Dutartre, M., Bayardon, J., and Jugé, S. (2016). Applications and stereoselective syntheses of *P*-chirogenic phosphorus compounds. Chem. Soc. Rev. *45*, 5771–5794.

13. Xiao, Y., Sun, Z., Guo, H., and Kwon, O. (2014). Chiral phosphines in nucleophilic organocatalysis. Beilstein J. Org. Chem. *10*, 2089–2121.

14. Guo, H., Fan, Y.C., Sun, Z., Wu, Y., and Kwon, O. (2018). Phosphine Organocatalysis. Chem. Rev. *118*, 10049–10293.

15. Lühr, S., Holz, J., and Börner, A. (2011). The synthesis of chiral phosphorus ligands for use in homogeneous metal catalysis. ChemCatChem *3*, 1708–1730.

16. Holshue, M.L., DeBolt, C., Lindquist, S., Lofy, K.H., Wiesman, J., Bruce, H., Spitters, C., Ericson, K., Wilkerson, S., Tural, A., et al.; Washington State 2019-nCoV Case Investigation Team (2020). First case of 2019 novel coronavirus in the United States. N. Engl. J. Med. *382*, 929–936.

17. Sun, Y., and Cramer, N. (2017). Rhodium(III)-catalyzed enantiotopic C−H activation enables access to *P*-chiral cyclic phosphinamides. Angew. Chem. Int. Ed. Engl. *56*, 364–367.

18. Zhu, R.-Y., Chen, L., Hu, X.-S., Zhou, F., and Zhou, J. (2019). Enantioselective synthesis of *P*-chiral tertiary phosphine oxides with an ethynyl group *via* Cu(i)-catalyzed azide-alkyne cycloaddition. Chem. Sci. (Camb.) *11*, 97–106.

19. Zheng, Y., Guo, L., and Zi, W. (2018). Enantioselective and regioselective hydroetherification of alkynes by gold-catalyzed desymmetrization of prochiral phenols with *P*-stereogenic centers. Org. Lett. *20*, 7039–7043.

20. Zhang, Y., Zhang, F., Chen, L., Xu, J., Liu, X., and Feng, X. (2019). Asymmetric synthesis of *P*-stereogenic compounds via Thulium(III)-catalyzed desymmetrization of dialkynylphosphine oxides. ACS Catal. *9*, 4834–4840.

21. Lin, Z.-Q., Wang, W.-Z., Yan, S.-B., and Duan, W.-L. (2015). Palladium-catalyzed enantioselective C-H arylation for the synthesis of *P*-stereogenic compounds. Angew. Chem. Int. Ed. Engl. *54*, 6265–6269.

22. Du, Z.-J., Guan, J., Wu, G.-J., Xu, P., Gao, L.-X., and Han, F.-S. (2015). Pd(II)-catalyzed enantioselective synthesis of *P*-stereogenic phosphinamides via desymmetric C-H arylation. J. Am. Chem. Soc. *137*, 632–635.

23. Liu, L., Zhang, A.-A., Wang, Y., Zhang, F., Zuo, Z., Zhao, W.-X., Feng, C.-L., and Ma, W. (2015). Asymmetric synthesis of *P*-stereogenic phosphinic amides via Pd(0)-catalyzed enantioselective intramolecular C–H arylation. Org. Lett. *17*, 2046–2049.

24. Huang, Z., Huang, X., Li, B., Mou, C., Yang, S., Song, B.-A., and Chi, Y.R. (2016). Access to *P*-stereogenic phosphinates via *N*-heterocyclic carbene-catalyzed desymmetrization of bisphenols. J. Am. Chem. Soc. *138*, 7524–7527.

25. Wang, Z., and Hayashi, T. (2018). Rhodium-catalyzed enantioposition-selective hydroarylation of divinylphosphine oxides with aryl boroxines. Angew. Chem. Int. Ed. Engl. *57*, 1702–1706.

26. Yang, G.-H., Li, Y., Li, X., and Cheng, J.-P. (2019). Access to P-chiral phosphine oxides by enantioselective allylic alkylation of bisphenols. Chem. Sci. (Camb.) *10*, 4322–4327.

27. Jang, Y.-S., Dieckmann, M., and Cramer, N. (2017). Cooperative effects between chiral Cpx–iridium(III) catalysts and chiral carboxylic acids in enantioselective C−H amidations of phosphine oxides. Angew. Chem. Int. Ed. Engl. *56*, 15088–15092.

28. Harvey, J.S., Malcolmson, S.J., Dunne, K.S., Meek, S.J., Thompson, A.L., Schrock, R.R., Hoveyda, A.H., and Gouverneur, V. (2009). Enantioselective synthesis of *P*-stereogenic phosphinates and phosphine oxides by molybdenum-catalyzed asymmetric ring-closing metathesis. Angew. Chem. Int. Ed. Engl. *48*, 762–766.

29. Nishida, G., Noguchi, K., Hirano, M., and Tanaka, K. (2008). Enantioselective synthesis of *P*-stereogenic alkynylphosphine oxides by Rh-catalyzed [2+2+2] cycloaddition. Angew. Chem. Int. Ed. Engl. *47*, 3410–3413.

30. Genet, C., Canipa, S.J., O'Brien, P., and Taylor, S. (2006). Catalytic asymmetric synthesis of ferrocenes and *P*-stereogenic bisphosphines. J. Am. Chem. Soc. *128*, 9336–9337.

31. Genov, G.R., Douthwaite, J.L., Lahdenperä, A.S.K., Gibson, D.C., and Phipps, R.J. (2020). Enantioselective remote C-H activation directed by a chiral cation. Science *367*, 1246–1251.

32. Huang, Q.-H., Zhou, Q.-Y., Yang, C., Chen, L., Cheng, J.-P., and Li, X. (2021). Access to *P*-stereogenic compounds *via* desymmetrizing enantioselective bromination. Chem. Sci. (Camb.) *12*, 4582–4587.

33. Sun, Y., and Cramer, N. (2018). Tailored trisubstituted chiral Cp$^{\times}$Rh^{III} catalysts for kinetic resolutions of phosphinic amides. Chem. Sci. (Camb.) *9*, 2981–2985.

34. Fernández-Pérez, H., and Vidal-Ferran, A. (2019). Stereoselective catalytic synthesis of *P*-stereogenic oxides via hydrogenative kinetic resolution. Org. Lett. *21*, 7019–7023.

35. Qiu, H., Dai, Q., He, J., Li, W., and Zhang, J. (2020). Access to *P*-chiral *sec*- and *tert*-phosphine oxides enabled by Le-Phos-catalyzed asymmetric kinetic resolution. Chem. Sci. (Camb.) *11*, 9983–9988.

36. Liu, X.-T., Zhang, Y.-Q., Han, X.-Y., Sun, S.-P., and Zhang, Q.-W. (2019). Ni-catalyzed asymmetric allylation of secondary phosphine oxides. J. Am. Chem. Soc. *141*, 16584–16589.

37. Beaud, R., Phipps, R.J., and Gaunt, M.J. (2016). Enantioselective Cu-catalyzed arylation of secondary phosphine oxides with diaryliodonium salts toward the synthesis of *P*-chiral phosphines. J. Am. Chem. Soc. *138*, 13183–13186.

38. Dai, Q., Li, W., Li, Z., and Zhang, J. (2019). *P*-chiral phosphines enabled by palladium/Xiao-Phos-catalyzed asymmetric P-C cross-coupling of secondary phosphine oxides and aryl bromides. J. Am. Chem. Soc. *141*, 20556–20564.

39. Chan, V.S., Stewart, I.C., Bergman, R.G., and Toste, F.D. (2006). Asymmetric catalytic synthesis of *P*-stereogenic phosphines via a nucleophilic ruthenium phosphido complex. J. Am. Chem. Soc. *128*, 2786–2787.

40. Chan, V.S., Chiu, M., Bergman, R.G., and Toste, F.D. (2009). Development of ruthenium catalysts for the enantioselective synthesis of *P*-stereogenic phosphines via nucleophilic phosphido intermediates. J. Am. Chem. Soc. *131*, 6021–6032.

41. Chan, V.S., Bergman, R.G., and Toste, F.D. (2007). Pd-catalyzed dynamic kinetic enantioselective arylation of silylphosphines. J. Am. Chem. Soc. *129*, 15122–15123.

42. Scriban, C., and Glueck, D.S. (2006). Platinum-catalyzed asymmetric alkylation of secondary phosphines: enantioselective synthesis of *p*-stereogenic phosphines. J. Am. Chem. Soc. *128*, 2788–2789.

43. Huang, Y., Li, Y., Leung, P.-H., and Hayashi, T. (2014). Asymmetric synthesis of *P*-stereogenic diarylphosphinites by palladium-catalyzed enantioselective addition of diarylphosphines to benzoquinones. J. Am. Chem. Soc. *136*, 4865–4868.

44. Yang, Z., Gu, X., Han, L.-B., and Wang, J.J. (2020). Palladium-catalyzed asymmetric hydrophosphorylation of alkynes: facile access to *P*-stereogenic phosphinates. Chem. Sci. (Camb.) *11*, 7451–7455.

45. Balázs, L.B., Huang, Y., Khalikuzzaman, J.B., Li, Y., Pullarkat, S.A., and Leung, P.-H. (2020). Catalytic asymmetric diarylphosphine addition to α-diazoesters for the synthesis of *P*-stereogenic phosphinates via P*-N bond formation. J. Org. Chem. *85*, 14763–14771.

46. Dai, Q., Liu, L., Qian, Y., Li, W., and Zhang, J. (2020). Construction of P-chiral alkenylphosphine oxides through highly chemo-, regio-, and enantioselective hydrophosphinylation of alkynes. Angew. Chem. Int. Ed. Engl. *59*, 20645–20650.

47. DiRocco, D.A., Ji, Y., Sherer, E.C., Klapars, A., Reibarkh, M., Dropinski, J., Mathew, R., Maligres, P., Hyde, A.M., Limanto, J., et al. (2017). A multifunctional catalyst that stereoselectively assembles prodrugs. Science *356*, 426–430.

48. Knouse, K.W., deGruyter, J.N., Schmidt, M.A., Zheng, B., Vantourout, J.C., Kingston, C., Mercer, S.E., Mcdonald, I.M., Olson, R.E., Zhu, Y., et al. (2018). Unlocking P(V): Reagents for chiral phosphorothioate synthesis. Science *361*, 1234–1238.

49. Lemouzy, S., Giordano, L., Herault, D., and Buono, G. (2020). Introducing chirality at phosphorus atoms: an update on the recent synthetic strategies for the preparation of optically pure *P*-stereogenic molecules. Eur. J. Org. Chem. *2020*, 3351–3366.

50. Chen, L., Liu, X.-Y., and Zou, Y.-X. (2020). Recent advances in the construction of phosphorus-substituted heterocycles, 2009-2019. Adv. Synth. Catal. *362*, 1724–1818.

51. Glueck, D.S. (2008). Catalytic asymmetric synthesis of chiral phosphanes. Chemistry *14*, 7108–7117.

52. Trost, B.M., Spohr, S.M., Rolka, A.B., and Kalnmals, C.A. (2019). Desymmetrization of phosphinic acids via Pd-catalyzed asymmetric allylic alkylation: rapid access to *P*-chiral phosphinates. J. Am. Chem. Soc. *141*, 14098–14103.

53. Lim, K.M.-H., and Hayashi, T. (2017). Dynamic kinetic resolution in rhodium-catalyzed asymmetric arylation of phospholene oxides. J. Am. Chem. Soc. *139*, 8122–8125.

54. Toda, Y., Pink, M., and Johnston, J.N. (2014). Brønsted acid catalyzed phosphoramidic acid additions to alkenes: diastereo- and enantioselective halogenative cyclizations for the synthesis of *C*- and *P*-chiral phosphoramidates. J. Am. Chem. Soc. *136*, 14734–14737.

55. Fu, X., Loh, W.-T., Zhang, Y., Chen, T., Ma, T., Liu, H., Wang, J., and Tan, C.-H. (2009). Chiral guanidinium salt catalyzed enantioselective phospha-Mannich reactions. Angew. Chem. Int. Ed. Engl. *48*, 7387–7390.

56. Teo, R.H.X., Chen, H.J., Li, Y., Pullarkat, S.A., and Leung, P.-H. (2020). Asymmetric catalytic 1,2-dihydrophosphination of secondary 1,2-diphosphines-direct access to free P*- and P*,C*-diphosphines. Adv. Synth. Catal. *362*, 2373–2378.

57. Yue, W.-J., Xiao, J.-Z., Zhang, S., and Yin, L. (2020). Rapid synthesis of chiral 1,2-bisphosphine derivatives through copper(I)-catalyzed asymmetric conjugate hydrophosphination. Angew. Chem. Int. Ed. Engl. *59*, 7057–7062.

58. de Azambuja, F., Carmona, R.C., Chorro, T.H.D., Heerdt, G., and Correia, C.R.D. (2016). Noncovalent substrate-directed enantioselective heck reactions: synthesis of *S*- and *P*-stereogenic heterocycles. Chemistry *22*, 11205–11209.

59. Hamada, T., and Buchwald, S.L. (2002). *P*-chirogenic binaphthyl-substituted monophosphines: synthesis and use in enolate vinylation/arylation reactions. Org. Lett. *4*, 999–1001.

60. Li, Y.-B., Tian, H., and Yin, L. (2020). Copper(I)-catalyzed asymmetric 1,4-conjugate hydrophosphination of α,β-unsaturated amides. J. Am. Chem. Soc. *142*, 20098–20106.

61. Wang, C., Huang, K., Ye, J., and Duan, W.-L. (2021). Asymmetric synthesis of P-stereogenic secondary phosphine-boranes by an unsymmetric bisphosphine pincer-nickel complex. J. Am. Chem. Soc. *143*, 5685–5690.

62. Sun, C., Qi, X., Min, X.-L., Bai, X.-D., Liu, P., and He, Y. (2020). Asymmetric allylic substitution-isomerization to axially chiral enamides *via* hydrogen-bonding assisted central-to-axial chirality transfer. Chem. Sci. (Camb.) *11*, 10119–10126.

63. Wang, J., Qi, X., Min, X.-L., Yi, W., Liu, P., and He, Y. (2021). Tandem iridium catalysis as a general strategy for atroposelective construction of axially chiral styrenes. J. Am. Chem. Soc. *143*, 10686–10694.

64. Bai, X.-d., Wang, J., and He, Y. (2019). Iridium-catalyzed propenylation reactions for the synthesis of 4-pyridone derivatives. Adv. Synth. Catal. *361*, 496–501.

65. Takeuchi, R., and Kezuka, S. (2006). Iridium-catalyzed formation of carbon-carbon and carbon-heteroatom bonds. Synthesis *38*, 3349–3366.

66. Hartwig, J.F., and Stanley, L.M. (2010). Mechanistically driven development of iridium catalysts for asymmetric allylic substitution. Acc. Chem. Res. *43*, 1461–1475.

67. Tosatti, P., Nelson, A., and Marsden, S.P. (2012). Recent advances and applications of iridium-catalysed asymmetric allylic substitution. Org. Biomol. Chem. *10*, 3147–3163.

68. Liu, X.-J., Zheng, C., Yang, Y.-H., Jin, S., and You, S.-L. (2019). Iridium-catalyzed asymmetric allylic aromatization reaction. Angew. Chem. Int. Ed. Engl. *58*, 10493–10499.

69. Hethcox, J.C., Shockley, S.E., and Stoltz, B.M. (2016). Iridium-catalyzed diastereo-, enantio-, and regioselective allylic alkylation with prochiral enolates. ACS Catal. *6*, 6207–6213.

70. Qu, J., and Helmchen, G. (2017). Applications of iridium-catalyzed asymmetric allylic substitution reactions in target-oriented synthesis. Acc. Chem. Res. *50*, 2539–2555.

71. Cheng, Q., Tu, H.-F., Zheng, C., Qu, J.-P., Helmchen, G., and You, S.-L. (2019). Iridium-catalyzed asymmetric allylic substitution reactions. Chem. Rev. *119*, 1855–1969.

72. Rössler, S.L., Petrone, D.A., and Carreira, E.M. (2019). Iridium-catalyzed asymmetric synthesis of functionally rich molecules enabled by (phosphoramidite,olefin) ligands. Acc. Chem. Res. *52*, 2657–2672.

73. Scaringi, S., and Mazet, C. (2021). Kinetically controlled stereoselective access to branched 1,3-dienes by Ru-catalyzed remote conjugative isomerization. ACS Catal. *11*, 7970–7977.

74. Marsden, S.R., Mestrom, L., McMillan, D.G.G., and Hanefeld, U. (2020). Thermodynamically and kinetically controlled reactions in biocatalysis – from concepts to perspectives. Chemistry *12*, 426–437.

75. Clayden, J., Mitjans, D., and Youssef, L.H. (2002). Lithium-sulfoxide-lithium exchange for the asymmetric synthesis of atropisomers under thermodynamic control. J. Am. Chem. Soc. *124*, 5266–5267.

76. Clayden, J., and Lai, L.W. (2001). (−)-Ephedrine as an auxiliary for the asymmetric synthesis of atropisomeric amides by dynamic resolution under thermodynamic control. Tetrahedron Lett. *42*, 3163–3166.

77. Clayden, J.P., and Lai, L.W. (1999). Enantioselective synthesis of atropisomeric amides by dynamic resolution: thermodynamic control with a proline-derived diamine resolving agent. Angew. Chem. Int. Ed. Engl. *38*, 2556–2558.

78. Edwards, D.J., House, D., Sheldrake, H.M., Stone, S.J., and Wallace, T.W. (2007). Kinetic and thermodynamic control of axial chirality in biaryl-derived fused oxazolidine lactams exploiting a centre-axis relay of unit efficiency. Org. Biomol. Chem. *5*, 2658–2669.

79. Clayden, J., Senior, J., and Helliwell, M. (2009). Atropisomerism at C-S bonds: asymmetric synthesis of diaryl sulfones by dynamic resolution under thermodynamic control. Angew. Chem. Int. Ed. Engl. *48*, 6270–6273.

80. Clayden, J., Fletcher, S.P., McDouall, J.J.W., and Rowbottom, S.J.M. (2009). Controlling axial conformation in 2-arylpyridines and 1-arylisoquinolines: application to the asymmetric synthesis of QUINAP by dynamic thermodynamic resolution. J. Am. Chem. Soc. *131*, 5331–5343.

81. Betson, M.S., Clayden, J., Helliwell, M., and Mitjans, D. (2005). Kinetic and thermodynamic stereocontrol in the atroposelective formation of sulfoxides by oxidation of 2-sulfanyl-1-naphthamides. Org. Biomol. Chem. *3*, 3898–3904.

82. Kumarasamy, E., Raghunathan, R., Sibi, M.P., and Sivaguru, J. (2015). Nonbiaryl and heterobiaryl atropisomers: Molecular templates with promise for atropselective chemical transformations. Chem. Rev. *115*, 11239–11300.

83. Zhao, Y., and Truhlar, D.G. (2007). The Mo6 suite of density functionals for main group thermochemistry, thermochemical kinetics, noncovalent interactions, excited states, and transition elements: two new functionals and systematic testing of four Mo6-class functionals and 12 other functionals. Theor. Chem. Acc. *120*, 215–241.

84. Riplinger, C., and Neese, F. (2013). An efficient and near linear scaling pair natural orbital based local coupled cluster method. J. Chem. Phys. *138*, 034106–034118.

85. Riplinger, C., Sandhoefer, B., Hansen, A., and Neese, F. (2013). Natural triple excitations in local coupled cluster calculations with pair natural orbitals. J. Chem. Phys. *139*, 134101–134113.

86. Riplinger, C., Pinski, P., Becker, U., Valeev, E.F., and Neese, F. (2016). Sparse maps–A systematic infrastructure for reduced-scaling electronic structure methods. II. Linear scaling domain based pair natural orbital coupled cluster theory. J. Chem. Phys. *144*, 024109–024110.

87. Marenich, A.V., Cramer, C.J., and Truhlar, D.G. (2009). Universal solvation model based on solute electron density and on a continuum model of the solvent defined by the bulk dielectric constant and atomic surface tensions. J. Phys. Chem. B *113*, 6378–6396.

88. Hunter, C.A., and Sanders, J.K.M. (1990). The nature of. pi.-.pi. interactions. J. Am. Chem. Soc. *112*, 5525–5534.

89. Sinnokrot, M.O., Valeev, E.F., and Sherrill, C.D. (2002). Estimates of the ab initio limit for π-π interactions: the benzene dimer. J. Am. Chem. Soc. *124*, 10887–10893.

90. Wheeler, S.E., and Bloom, J.W.G. (2014). Toward a more complete understanding of noncovalent interactions involving aromatic rings. J. Phys. Chem. A *118*, 6133–6147.